Chapter 2
Power System Voltage Stability and Models of Devices

Abstract This chapter introduces the concepts of voltage instability and the distinctions between voltage and angle instability. The driving force and main causes of voltage instability are analysed. Different methods and devices used to enhance voltage stability are also explained. The steady-state and dynamic modelling of the power system devices including wind generators and photovoltaic units have been discussed.

2.1 Introduction

Power system stability has been recognised as an important problem for secure system operation since the beginning of last century. Many major blackouts caused due to power system instability have illustrated the importance of this phenomenon [1, 2]. Angle stability had been the primary concern of the utilities for many decades. However, in the last two decades power systems have operated under much more stressed conditions than they usually had in the past. There are number of factors responsible for this: continuing growth in interconnections; the use of new technologies; bulk power transmissions over long transmission lines; environmental pressures on transmission expansion; increased electricity consumption in heavy load areas (where it is not feasible or economical to install new generating plants); new system loading patterns due to the opening up of the electricity market; growing use of induction machines; and large penetration of wind generators and local uncoordinated controls in systems. Under these stressed conditions a power system can exhibit a new type of unstable behaviour, namely, voltage instability.

In recent years, voltage instability has become a major research area in the field of power systems after a number of voltage instability incidents were experienced around the world [3, 4]. In Japan, a large-scale power failure occurred in the Tokyo metropolitan area in 1987 (about an 8-GW loss) because of voltage instability [5]. In Tokyo, the capacitance of 275-kV underground cables created adverse effects on

J. Hossain and H. R. Pota, *Robust Control for Grid Voltage Stability: High Penetration of Renewable Energy*, Power Systems,
DOI: 10.1007/978-981-287-116-9_2,

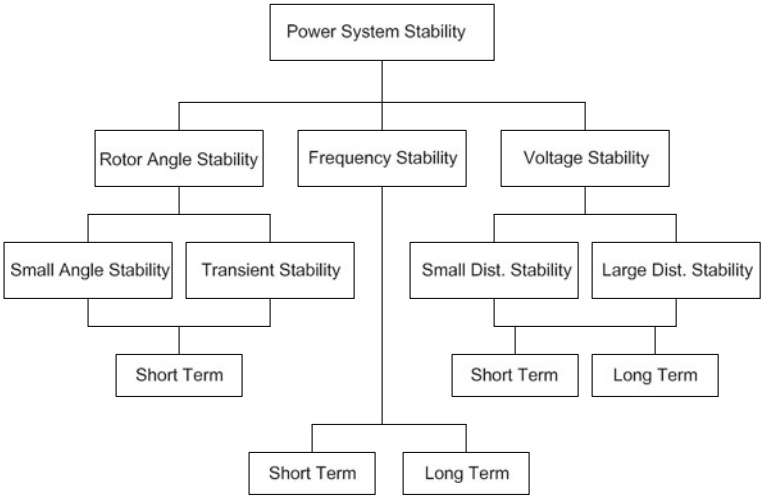

Fig. 2.1 Classification of power system stability

voltage-stability characteristics, making voltage stability one of the most important issues regarding system security. It has even been suggested that part of the problems that led to the North American blackout of August 2003 might be linked to short-term voltage instability [6]. In recent years, voltage instability has been responsible for several network collapses and blackouts [7] and is now receiving special attention in many systems.

This chapter will provide an overview of voltage stability problems and methods of effectively addressing them in the design and operation of electrical power systems. This includes the basic concepts, physical aspects of the phenomenon, methods of analysis, examples of major power grid blackouts due to voltage instability and methods of preventing voltage instability. This chapter addresses issues of power system voltage stability and identifies different categories of voltage stability behaviour that are important in power system stability analyses. In addition, the modeling of power system devices under consideration will be discussed.

2.2 Power System Stability and Voltage Stability

Power system stability is the ability of an electrical power system, for given initial operating conditions, to regain a state of operating equilibrium after being subjected to a physical disturbance, with most system variables bounded so that practically the entire system remains intact. Figure 2.1 gives the overall picture of the power system stability problem, identifying its categories and subcategories.

The concept of voltage stability addresses a large variety of different phenomena depending on which part of the power system is being analysed; for instance, it can be a fast phenomenon if induction motors, air conditioning loads or high-voltage DC transmission (HVDC) links are involved or a slow phenomenon if, for example, a mechanical tap changer is involved. Today, it is well accepted that voltage instability is a dynamic process since it is related to dynamic loads [8, 9].

Voltage stability refers to the ability of a power system to maintain steady voltages at all buses in the system and maintain or restore equilibrium between load demand and load supply from its given initial operating conditions after it has been subjected to a disturbance. Instability may result in progressive voltage falls or rises at some buses. A possible outcome of voltage instability is the loss of load in an area, and possible tripping of transmission lines and other elements by their protective systems which can lead to cascading outages.

Voltage collapse is more complex than voltage instability and is the process by which the sequence of events accompanying voltage instability lead to a blackout or abnormally low voltages in a significant part of a power system. The main symptoms of voltage collapse are: low voltage profiles; heavy reactive power flows; inadequate reactive support; and heavily loaded systems. The collapse is often precipitated by low-probability single or multiple contingencies. When a power system is subjected to a sudden increase of reactive power demand following a system contingency, the additional demand is met by the reactive power reserves of generators and compensators. Generally, there are sufficient reserves and the system settles to a stable voltage level. However, it is possible, due to a combination of events and system conditions, that the lack of additional reactive power may lead to voltage collapse, thereby causing a total or partial breakdown of the system.

2.3 Voltage and Angle Instability

Power system instability is essentially a single problem; however, the various forms of instability that a power system may undergo cannot be properly understood and effectively dealt with by treating it as such. Because of the high dimensionality and complexity of stability problems, it helps to simplify models in order to analyse specific types of problems using an appropriate degree of detail of the system representation and appropriate analytical techniques.

There is no clear distinction between voltage and angle instability problems but, in some circumstances, one form of instability predominates over the other. Distinguishing between the two types is important for understanding their underlying causes in order to develop appropriate design and operating procedures but, although this is effective, the overall stability of the system should be kept in mind. Solutions for one problem should not be at the expense of another. It is essential to look at all aspects of the stability phenomena and at each aspect from more than one viewpoint.

However, there are many cases, in which, one form of instability predominates. An IEEE report [10] points out the extreme situations of: (1) a remote synchronous

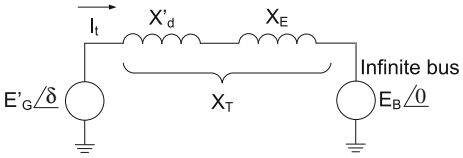

Fig. 2.2 Pure angle stability

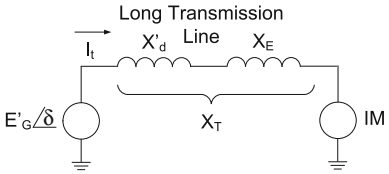

Fig. 2.3 Pure voltage stability

generator connected by transmission lines to a large system–angle stability dominates (one machine to an infinite-bus problem); and (2) a synchronous generator or large system connected by long transmission lines to an asynchronous load–voltage stability dominates. Figures 2.2 and 2.3 show these extremes. Details of the relationship between voltage and angle stability are given in [11].

Voltage stability is concerned with load areas and load characteristics. For rotor angle stability, we are often concerned with integrating remote power plants to a large system over long transmission lines. Basically, voltage stability is load stability and rotor angle stability is generator stability. In a large interconnected system, voltage collapse of a load area is possible without the loss of synchronism of any generator. Transient voltage stability is usually closely associated with transient rotor angle stability but longer-term voltage stability is less linked with rotor angle stability. It can be said that if voltage collapses at a point in a transmission system remote from the load, it is an angle instability problem. If it collapses in a load area, it is mainly a voltage instability problem.

2.4 Wind Power Generation and Power System Stability

In most countries, the amount of wind power generation integrated into large-scale electrical power systems is only a small part of the total power system load. However, the amount of electricity generated by wind turbines (WTs) is continuously increasing. Therefore, wind power penetration in electrical power systems will increase in future and will start to replace the output of conventional synchronous generators. As a result, it may also begin to influence overall power system behaviour. WTs use generators, such as squirrel-cage induction generators (IGs) or generators that are grid-coupled via power electronic converters. The interactions of these generator

types with the power system are different from that of a conventional synchronous generator. As a consequence, WTs affect the dynamic behaviour of a power system in a way that might be different from that of synchronous generators. Therefore, the impact of wind power on the dynamics of power systems should be studied thoroughly in order to identify potential problems and to develop measures to mitigate those problems.

In grid impact studies of wind power integration, voltage stability is the main problem that will affect the operation and security of wind farms and power grids [12]. Voltage stability deterioration is mainly due to the large amount of reactive power absorbed by the WTs during their continuous operation and system contingencies. The various WT types presently in use behave differently during grid disturbances. Induction generators consume reactive power and behave similarly to induction motors for the duration of system contingency and will deteriorate the local grid voltage stability. Also, variable-speed wind turbines (VSWTs) equipped with doubly-fed induction generators (DFIGs) are becoming more widely used for their advanced reactive power and voltage control capability. DFIGs make use of power electronic converters and are, thus, able to regulate their own reactive power so as to operate at a given power factor or to control grid voltage. But, because of the limited capacity of a pulse-width modulation (PWM) converter [13], the voltage control capability of a DFIG cannot match with that of a synchronous generator. When the voltage control requirement is beyond the capability of a DFIG, the voltage stability of the grid is also affected.

When dealing with power system stability and wind power generation these questions may be raised, How does wind power generation contribute to power system stability? What are the factors that limit the integration of WTs into existing power systems? How many additional wind generators can be integrated by using static and dynamic compensations? Some cases of system stability problems related to wind power generation are presented in this book.

2.5 Voltage Instability and Time Frame of Interest

The time-frame of interest for voltage stability problems may vary from a few seconds to tens of minutes. Therefore, voltage stability may be either a short- or long-term phenomenon. Short-term voltage stability involves the dynamics of fast-acting load components such as induction motors, electronically controlled loads and HVDC converters. The study period of interest here is in the order of several seconds, and any analysis requires solutions of the appropriate system differential equations; this is similar to the analysis of rotor angle stability. Dynamic modeling of loads is often essential. In contrast to angle stability, short-circuits near loads are important.

Long-term voltage stability involves slower-acting equipment, such as tap-changing transformers, thermostatically controlled loads and generator current limiters. Here, the study period of interest may extend to several or many minutes, and long-term simulations are required for the analysis of a system's dynamic perfor-

mance [14]. Stability is usually determined by the resulting outage of equipment, rather than the severity of the initial disturbance. Instability is due to the loss of long-term equilibrium (e.g., when loads try to restore their power beyond the capability of the transmission network and connected generation), the post-disturbance steady-state operating point being small-disturbance unstable, and/or a lack of attraction toward the stable post-disturbance equilibrium (e.g., when a remedial action is applied too late) [15, 16]. The disturbance could also be a sustained load build-up (e.g., motoring load increase).

Large-disturbance voltage stability refers to a system's ability to maintain steady voltages following large disturbances, such as system faults, loss of generation or circuit contingencies. This ability is determined by the system and load characteristics, and the interactions of both continuous and discrete controls and protections. Determination of large-disturbance voltage stability requires the examination of the nonlinear response of the power system over a period of time sufficient to capture the performance and interactions of such devices as motors, underload transformer tap changers and generator field-current limiters. The study period of interest may extend from a few seconds to tens of minutes.

Small-disturbance voltage stability refers to a system's ability to maintain steady voltages when subjected to small perturbations, such as incremental changes in system load. This form of stability is influenced by the characteristics of loads, continuous controls and discrete controls at a given instant of time. This concept is useful for determining, at any instant, how the system voltages will respond to small system changes. With appropriate assumptions, system equations can be linearised for analysis, thereby allowing the computation of valuable sensitivity information which is useful for identifying the factors influencing stability. However, this linearisation cannot account for nonlinear effects, such as tap-changer controls (dead-bands, discrete tap steps, and time delays). Therefore, a combination of linear and nonlinear analyses can be used in a complementary manner [8] to study voltage stability.

2.6 Voltage Stability

The practical importance of voltage stability analysis is that it helps in designing and selecting countermeasures which will avoid voltage collapse and enhance stability. Voltage stability analysis has gained increasingly importance in recent years due to:

- generation being centralised in fewer, larger power plants which means fewer voltage-controlled buses, and longer electrical distances between generation and load;
- the integration of large-scale induction generators;
- the extensive use of shunt capacitor compensation;
- voltage instability caused by line and generator outages;
- many incidents having occurred throughout the world (France, Belgium, Sweden, Japan, USA, etc) [3, 4]; and
- the operation of a system being closer to its limits.

2.7 Voltage Stability and Nonlinearity

Historically, power systems were designed and operated conservatively. It was comparatively easy to match load growth with new generation and transmission equipment. So, systems were operated in regions where behaviour was fairly linear. Only occasionally would systems be forced to extremes where nonlinearities could begin to have significant effects. However, the recent trend is for power systems to be operated closer to their limits. Also, as the electricity industry moves towards an open-access market, operating strategies will become much less predictable. Hence, the reliance on fairly linear behaviour which was adequate in the past, must give way to an acceptance that nonlinearities are going to play an increasingly important role in power system operation.

One important aspect of the voltage stability problem, making its understanding and solution more difficult, is that the phenomena involved are truly nonlinear. As the stress on a system increases, this nonlinearity becomes more and more pronounced. The nonlinearity of loads and generator dynamics are important factors when determining voltage instability. Therefore, it is essential that the nonlinear behaviour of power system devices should be taken into account when designing controllers and analysing dynamic behaviours.

2.8 Main Causes of Voltage Instability

The driving force for voltage instability is usually the loads; in response to a disturbance, power consumed by the loads tends to be restored by the action of motor slip adjustment, distribution voltage regulators, tap-changing transformers and thermostats. Restored loads increase the stress on a high-voltage network by increasing the reactive power consumption and causing further voltage reduction. A run-down situation causing voltage instability occurs when load dynamics attempt to restore power consumption beyond the capability of the transmission network and the connected generation [15–18].

A major factor contributing to voltage instability is the voltage drop that occurs when both active and reactive power flow through the inductive reactances of a transmission network; this limits the capabilities of the transmission network, in terms of power transfer and voltage support, which are further limited when some of the generators hit their field, or armature current, time-overload capability limits. It is worth noting that, in almost all voltage instability incidents, one or several crucial generators were operating with a limited reactive capability [16]. Voltage stability is threatened when a disturbance increases the reactive power demand beyond the sustainable capacity of the available reactive power resources.

While the most common form of voltage instability is progressive drops in bus voltages, the risk of over-voltage instability also exists and has been experienced in at least one system [19]. This is caused by the capacitive behaviour of a network

(EHV transmission lines operating below surge impedance loading) as well as by underexcitation limiters preventing generators and/or synchronous compensators from absorbing the excess reactive power. In this case, instability is associated with the inability of the combined generation and transmission systems to operate below some load level. In their attempt to restore this load power, transformer tap changers may cause long-term voltage instability.

Voltage stability problems may also be experienced at the terminals of HVDC links used for either long-distance or back-to-back applications [20]. They are usually associated with HVDC links connected to weak AC systems and may occur at rectifier or inverter stations, and are associated with the unfavourable reactive power load characteristics of converters. A HVDC link's control strategies have a very significant influence on such problems, since the active and reactive power at the AC/DC junction is determined by the controls. If the resulting loading on an AC transmission stresses it beyond its capability, voltage instability occurs. Such a phenomenon is relatively fast with the time frame of interest being in the order of one second or less. Voltage instability may also be associated with converter transformer tap-changer controls which is a considerably slower phenomenon. Recent developments in HVDC technology (voltage-source converters and capacitor-commutated converters) have significantly increased the limits for the stable operation of HVDC links in weak systems compared with the limits for line-commutated converters.

One form of the voltage stability problem, that results in uncontrolled over-voltages, is the self-excitation of synchronous machines. This can arise if the capacitive load of a synchronous machine is too large. Examples of excessive capacitive loads that can initiate self-excitation are open-ended high-voltage lines, and shunt capacitors and filter banks from HVDC stations. The over-voltages that result when a generator load changes to a capacitive load are characterised by an instantaneous rise at the instant of change followed by a more gradual rise. This latter rise depends on the relationship between the capacitive load component and the machine reactance, together with the excitation system of the synchronous machine. The negative field current capability of an exciter is a feature that has a positive influence on its limits for self-excitation. A voltage collapse may be aggravated by the excessive use of shunt capacitor compensation, due to the inability of the system to meet its reactive demands, or large sudden disturbances, such as the loss of either a generating unit or a heavily loaded line, or cascading events or poor coordination between various control and protective systems.

2.9 Methods for Improving Voltage Stability

The control of voltage levels is accomplished by controlling the production, absorption and flow of reactive power at all levels in a system. In order to function properly, it is essential that the voltage is kept close to the nominal value throughout the entire power system. Traditionally, this has been achieved differently for transmission networks and distribution grids. In transmission networks, a large-scale

centralised power plant keeps the node voltages within an allowed deviation from their nominal values and the number of dedicated voltage control devices is limited.

In contrast, distribution grids incorporate dedicated equipment for voltage control and the generators connected to the distribution grid are hardly, if at all, involved in controlling the node voltages. The most frequently used voltage control devices in distribution grids are tap-changer transformers that change their turns ratio but switched capacitors and reactors are also applied. However, a number of recent developments challenge this traditional approach. One of these is the increased use of WTs for generating electricity. When large-scale wind farms are connected to the grids, it will be difficult to maintain node voltages using the traditional reactive power control devices. In these cases, some dedicated equipment, such as flexible AC transmission system (FACTS) devices will have to be used as well. FACTS devices offer fast and reliable control over the three AC transmission system parameters, i.e., voltage, line impedance and phase angle, and make it possible to control voltage stability dynamically.

2.9.1 Voltage Stability and Exciter Control

Automatic voltage regulators (AVRs) with synchronous machines are the most important means of voltage control in a power system. A synchronous machine is capable of generating and supplying reactive power within its capability limits to regulate system voltage. For this reason, it is an extremely valuable part of the solution to the collapse-mitigation problem.

The performance requirements of excitation systems are determined by considerations of the synchronous generator as well as the power system. The basic requirement is that the excitation system supplies and automatically adjusts the field current of the synchronous generator in order to maintain the scheduled terminal voltage as the output varies within the continuous capability of the generator. An excitation system must be able to respond to transient disturbances by field forcing consistent with the generator's instantaneous and short-term capabilities. The generator capability is limited by several factors: rotor insulation failure due to high field voltage; rotor heating due to high field current; stator heating due to high armature current loading; core end heating during underexcited operation; and heating due to excess flux (volts/Hz).

The role of an excitation system for enhancing power system performance has been continually growing. Early excitation systems were controlled manually to maintain the desired generator terminal voltage and reactive power loading. When the voltage control was first automated, it was very slow, basically filling the role of an alert operator [18]. Many research works have been undertaken in the area of voltage control using efficient excitation control. Modern excitation systems are capable of providing practically instantaneous responses with high ceiling voltages.

The combination of a high field-forcing capability and the use of auxiliary stabilising signals contributes to the substantial enhancement of overall system dynamic performance.

2.9.2 Voltage Stability and FACTS Devices

During the past two decades, the increase in electrical energy demand has presented higher requirements for the power industry. In recent years, the increases in peak load demands and power transfers between utilities have elevated concerns about system voltage security. Voltage instability is mainly associated with a reactive power imbalance. Improving a system's reactive power-handling capacity via FACTS devices is a remedy for the prevention of voltage instability and, hence, voltage collapse.

With the rapid development of power electronics, FACTS devices have been proposed and installed in power systems. They can be utilised to control power flow and enhance system stability. Particularly with the deregulation of the electricity market, there is an increasing interest in using FACTS devices for the operation and control of power systems with new loading and power flow conditions. For a better utilization of existing power systems, i.e., to increase their capacities and controllability, installing FACTS devices becomes imperative.

In the present situation, there are two main aspects that should be considered when using FACTS devices: the flexible power system operation according to their power flow control capability; and improvements in the transient and steady-state stability of power systems. FACTS devices are the right equipment to meet these challenges and different types are used in different power systems.

The most commonly used devices in present power grids are shunt capacitors and mechanically-controlled circuit breakers (MCCBs). Within limits, static reactive sources, such as shunt capacitors, can assist in voltage support. However, unless they are converted to pseudo-dynamic sources by being mechanically switched, they are not able to help support voltages during emergencies, when more reactive power support is required. In fact, shunt capacitors suffer from a serious drawback of providing less reactive support at the very time that more support is needed, i. e., during a voltage depression volt-ampere-reactive (VAr) output being proportional to the square of the applied voltage.

Long switching periods and discrete operation make it difficult for MCCBs to handle the frequently changing loads smoothly and damp out the transient oscillations quickly. In order to compensate for these drawbacks, large operational margins and redundancies are maintained in order to protect the system from dynamic variation and recover from faults. However, this not only increases the cost and lowers the efficiency, but also increases the complexity of a system and augments the difficulty of its operation and control. Severe black-outs in power grids which have happened recently worldwide have revealed that conventional transmission systems are unable to manage the control requirements of complicated interconnections and variable power flows.

More smoothly controlled, and faster, reactive support than mechanically switched capacitors can be provided by true dynamic sources of reactive power such as static VAr compensators (SVCs), static synchronous compensators (STATCOMs), synchronous condensers and generators. The application of SVCs and STATCOMs, in the context of voltage stability, has been discussed in recent literature [21]. The main differences between these two devices are that the SVC becomes a shunt capacitor when it reaches the limit of its control and all capacitance is fully switched in, and its reactive power output decreases as the square of the voltage when the maximum range of control is reached. The main advantage of the STATCOM over the thyristor type SVC is that the compensating current does not depend on the voltage level of the connecting point and thus the compensating current is not lowered as the voltage drops [22]. STATCOMs help to meet the wind farm interconnection standards and also provide dynamic voltage regulation, power factor correction and a low-voltage ride-through capability for an entire wind farm.

2.10 Modeling of Power System Devices

Power systems are large interconnected systems consisting of generation units, transmission grids, distribution systems and consumption units. The stability of a power system is dependent on several components, such as conventional generators and their exciters, wind generators, PV units, dynamic loads and FACTS devices. Therefore, an understanding of the characteristics of these devices and the modeling of their performances are of fundamental importance for stability studies and control design. There are numerous dynamics associated with a power system which may affect its large-signal stability and cause other kinds of stability problems. The large-signal stability technique analyses a system's stability by studying detailed simulations of its dynamics.

Modern power systems are characterised by complex dynamic behaviours which are due to their size and complexity. As the size of a power system increases, its dynamic processes become more challenging for analysis as well as for an understanding of its underlying physical phenomena. Power systems, even in their simplest form, exhibit nonlinear and time-varying behaviours. Moreover, there is a wide variety of equipment in today's power systems, namely: (1) synchronous generators, PV units and wind generators; (2) loads; (3) reactive-power control devices, such as capacitor banks and shunt reactors; (4) power-electronically switched devices, such as SVCs, and currently developed FACTS devices, such as STATCOMs; (5) series capacitors, thyristor-controlled series capacitors (TCSCs), among others. Though the kinds of equipment found in today's power systems are well-established and quite uniform in design, their precise modeling plays an important role in analysis and simulation studies of a whole system.

Different approaches to system modeling lead to different analytical results and accuracy. Improper models may result in over-estimated stability margins which can be disastrous for system operation and control. On the contrary, redundant models will

greatly increase computation costs and could be impractical for industrial application. To study the problem of modeling, all the components of a power system should be considered for their performance. Based on the requirements of stability study, different modeling schemes can be used for the same device; for example, three kinds of models of a system or device are necessary in order to study a power system's long term, midterm and transient stabilities.

Traditional system modeling has been based on generators and their controls as well as the transmission system components. Only recently load modeling has received more and more attention for stability analysis purposes. Test systems considered in this dissertation consist of conventional generators, wind generators, PV units, generator control systems including excitation control, automatic voltage regulators (AVRs), power system stabilisers (PSSs), transmission lines, transformers, reactive power compensation devices, newly developed FACTS devices and loads of different kinds. Each piece of equipment has its own dynamic properties that may need to be modelled for a stability study.

The dynamic behaviours of these devices are described through a set of nonlinear differential equations while the power flow in the network is represented by a set of algebraic equations. This gives rise to a set of differential-algebraic equations (DAEs) describing the behaviour of a power system. After suitable representations of these elements, one can arrive at a network model of a system in terms of its admittance matrix. Generally because of a large number of nodes in the system, this matrix will be large but can be reduced by making suitable assumptions. Different types of models have been reported in the literature for each type of power system component depending upon its specific applications [18]. In this chapter, the relevant equations governing the dynamic behaviours of the specific types of models used in this dissertation are described.

2.10.1 Modeling of Synchronous Generators

A synchronous machine is one of the most important power system components. It can generate active and reactive power independently and has an important role in voltage control. The synchronising torques between generators act to keep large power systems together and make all generator rotors rotate synchronously. This rotational speed is what determines the mains frequency which is kept very close to the nominal value of 50 or 60 Hz.

Generally, the well-established Park's model for a synchronous machine is used in system analysis. However, some modifications can be employed to simplify it for stability analysis. Depending on the nature of the study, several models of a synchronous generator, having different levels of complexity, can be utilised [18]. In the simplest case, a synchronous generator is represented by a second-order differential equation, while studying fast transients in a generator's windings requires the use of a more detailed model, e.g., a sub-transient 6*th*-order model. Throughout this book, sub-transient and third-order transient generator models are used.

The IEEE recommended practice regarding the d–q axis orientation of a synchronous generator is followed here [18]. This results in a negative d-axis component of stator current for an overexcited synchronous generator delivering power to the system. The differential equations, governing the sub-transient dynamic behaviour of generators in a multi-machine interconnected system, are given by [23]:

$$\dot{\delta}_k = \omega_k \omega_s - \omega_s, \tag{2.1}$$

$$\dot{\omega}_k = \frac{1}{2H_k}\left[T_{m_k} - \frac{X''_{d_k} - X_{ls_k}}{X'_{d_k} - X_{ls_k}} E'_{q_k} I_{q_k} - \frac{X'_{d_k} - X''_{d_k}}{X'_{d_k} - X_{ls_k}} \psi_{1d_k} I_{q_k} + \frac{X'_{q_k} - X''_{q_k}}{X'_{q_k} - X_{ls_k}} \psi_{2q_k} I_{d_k} - \frac{X''_{q_k} - X_{ls_k}}{X'_{q_k} - X_{ls_k}} E'_{d_k} I_{d_k} + (X''_{q_k} - X''_{d_k}) I_{q_k} I_{d_k} - D_k \omega_k\right], \tag{2.2}$$

$$\dot{E}'_{q_k} = \frac{1}{T'_{do_k}}\left[-E'_{q_k} - (X_{d_k} - X'_{d_k})\{-I_{d_k} - \frac{X'_{d_k} - X''_{d_k}}{(X'_{d_k} - X_{ls_k})^2}(\psi_{1d_k} - (X'_{d_k} - X_{ls_k}) I_{d_k} - E'_{q_k})\} + K_{a_k}(V_{ref_k} - V_{t_k} + V_{s_k})\right], \tag{2.3}$$

$$\dot{E}'_{d_k} = -\frac{1}{T'_{qo_k}}\left[E'_{d_k} + (X_{q_k} - X'_{q_k})\{I_{q_k} - \frac{X'_{q_k} - X''_{q_k}}{(X'_{q_k} - X_{ls_k})^2}(-\psi_{2q_k} + (X'_{q_k} - X_{ls_k}) I_{q_k} - E'_{d_k})\}\right], \tag{2.4}$$

$$\dot{\psi}_{1d_k} = \frac{1}{T''_{do_k}}\left[-\psi_{1d_k} + E'_{q_k} + (X_{d_k} - X_{ls_k}) I_{d_k}\right], \tag{2.5}$$

$$\dot{\psi}_{2q_k} = -\frac{1}{T''_{qo_k}}\left[\psi_{2q_k} + E'_{d_k} - (X_{q_k} - X_{ls_k}) I_{q_k}\right], \tag{2.6}$$

for $k = 1, 2, \ldots, m$, where m is the total number of generators, K_{a_k} the AVR gain, V_{ti_k} the terminal voltage, V_{s_k} the auxiliary input signal to the exciter, δ_k the power angle of the generator, ω_k the rotor speed with respect to a synchronous reference, E'_{q_k} the transient emf due to field flux linkage, E'_{d_k} the transient emf due to flux linkage in the d-axis damper coil, ψ_{1d_k} the sub-transient emf due to flux linkage in the d-axis damper, ψ_{2q_k} the sub-transient emf due to flux linkage in the q-axis damper, ω_s the absolute value of the synchronous speed in radians per second, H_k the inertia constant of the generator, D_k the damping constant of the generator, T'_{do_k} and T''_{do_k} the direct-axis open-circuit transient and sub-transient time constants, T'_{qo_k} and T''_{qo_k} the q-axes open-circuit transient and sub-transient time constants, I_{d_k} and I_{q_k} the d- and q-axes components of the stator current, X_{ls_k} the armature leakage reactance, X_{d_k}, X'_{d_k} and X''_{d_k} the synchronous, transient and sub-transient reactances along the d-axis, X_{q_k}, X'_{q_k} and X''_{q_k} the synchronous, transient and sub-transient reactances along the q-axis, respectively.

For stability analysis, the stator transients are assumed to be much faster compared to the swing dynamics [23]. Hence, the stator quantities are assumed to be related to the terminal bus quantities through algebraic equations rather than differential equations. The stator algebraic equation is given by:

$$V_i \cos(\delta_i - \theta_i) - \frac{X''_{d_i} - X_{ls_i}}{X'_{d_i} - X_{ls_i}} E'_{q_i} - \frac{X'_{d_i} - X''_{d_i}}{X'_{d_i} - X_{ls_i}} \psi_{1d_i} + R_{s_i} I_{q_i} - X''_{d_i} I_{d_i} = 0, \quad (2.7)$$

$$V_i \sin(\delta_i - \theta_i) + \frac{X''_{q_i} - X_{ls_i}}{X'_{q_i} - X_{ls_i}} E'_{d_i} - \frac{X'_{q_i} - X''_{q_i}}{X'_{q_i} - X_{ls_i}} \psi_{2q_i} - R_{s_i} I_{d_i} - X''_{q_i} I_{d_i} = 0, \quad (2.8)$$

where V_i is the generator terminal voltage. Under typical assumptions, the single-axis synchronous generator can be modeled by the following set of nonlinear differential equations [24]:

$$\dot{\delta}_k = \omega_k \omega_s - \omega_s, \quad (2.9)$$

$$\dot{\omega}_k = \frac{1}{2H_k} \left[P_{m_k} - E'_{q_k} I_{q_i} - D_k \omega \right], \quad (2.10)$$

$$\dot{E}'_{q_k} = \frac{1}{T'_{d0_k}} \left[E_{fd_k} - E'_{q_k} - (X_{d_k} - X'_{d_k}) I_{d_k} \right], \quad (2.11)$$

where E_{fd_i} is the equivalent emf in the exciter coil. The mechanical input power, P_{m_i}, to the generator is assumed to be constant.

2.10.2 Modeling of Excitation Systems

Control of the excitation system of a synchronous machine has a very strong influence on its performance, voltage regulation and stability [25]. Not only is the operation of a single machine affected by its excitation but, also, the behaviour of the whole system is dependent on the excitation system of the generators; for example, inter-area oscillations are directly connected to the excitations of the generators [26]. In general, the whole excitation control system includes:

- a PSS;
- an excitation system stabilizer;
- an AVR; and
- a terminal voltage transducer and load compensator.

There are different types of excitation systems commercially available in the power industry. However, one of the most commonly encountered models is the so-called IEEE Type ST1A excitation system. Other excitation system models for large-scale power system stability studies can be found in [27]. The main equations describing IEEE Type ST1A excitation are listed below:

$$\dot{V}_{tr_k} = \frac{1}{T_{r_k}} \left[-V_{tr_k} + V_{t_k} \right], \quad (2.12)$$

$$E_{fd_k} = K_{a_k} (V_{ref_k} - V_{tr_k}), \quad (2.13)$$

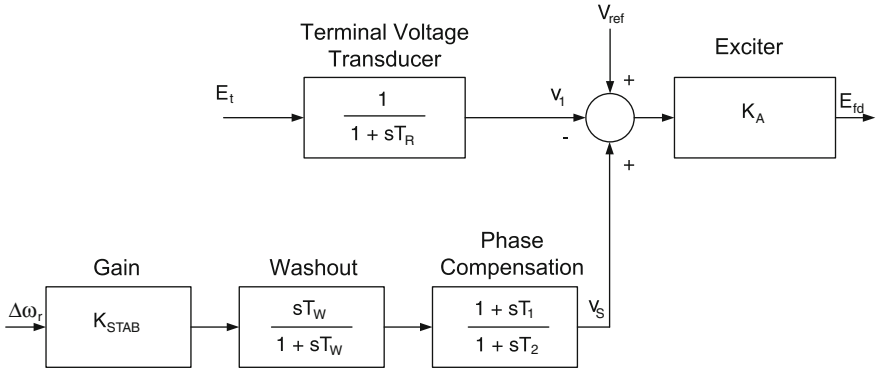

Fig. 2.4 PSS with AVR block diagram

where V_{tr_k} is the measured voltage state variable after the sensor lag block, V_{t_k} the measured terminal voltage, K_{a_k} the AVR gain and T_{r_k} the sensor time constant. In this dissertation, a robust excitation system is designed later and its performance is compared with that of the above excitation system.

2.10.3 Power System Stabilisers

The AVR plays an important role in keeping a generator synchronised with other generators in the grid. To achieve this, it should be fast-acting. Using high AVR gain to increase the action time often leads to unstable and oscillatory responses. To increase the damping of a lightly damped mode, the AVR uses a signal proportional to the rotor speed, although generator power and frequency may also be used [28]. The dynamic compensator used to modify the input signal to an AVR is commonly known as a PSS. Most generators have a PSS to improve stability and damp out oscillations.

Synchronous machines connected to a grid employ PSSs to enhance the damping of rotor oscillations. A typical PSS uses the change in speed, $\Delta\omega$, as the feedback variable and its output, V_s, is mixed with the reference voltage, V_{ref}, to produce the excitation signal. The block diagram in Fig. 2.4 shows the excitation system with an AVR and a PSS [18]. The amount of damping provided by a PSS depends on the value of the gain block, K_{STAB}. The phase compensation block introduces the phase lead necessary to compensate for the phase lag that is introduced between the exciter input and the generator electrical torque. The wash-out block serves as a high-pass filter, with the time constant, T_W, being high enough to allow signals associated with oscillations in ω_r to pass unchanged and block slowly varying speed changes. It allows the PSS to respond only to fast changes in speed.

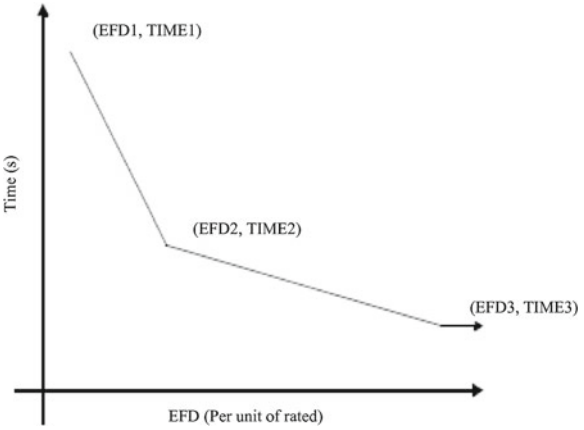

Fig. 2.5 Over-excitation limiter operating principle

2.10.4 Over-Excitation Limiters

An over-excitation limiter (OXL) can take two forms: (1) a device that limits the thermal duty of the rotor field circuit on a continuous current basis; and (2) a device that limits the effects of stator or transformer core iron saturation due to excessive generator terminal voltage, under-frequency, or the combination of both. An OXL to protect the rotor from thermal overload, is an important controller in system voltage stability. It is usually disabled in the transient time-frame to allow the excitation system to force several times the rated voltage across the rotor winding and more than the rated continuous current to help retain transient stability.

After a few seconds, the limiter is activated in an inverse time function–the higher the rotor current, the sooner the limiter is activated. This brings the continuous rotor current down to, or just below, the rated level to ensure the rotor is not overheated by excessive current. The limiter acts without regard to the actual rotor temperature. Even if the rotor is very cool before the over-excitation event, the time characteristic of the limiter is not changed. The over-excitation operating principle is shown in Fig. 2.5.

Note:

- below EFD1, the device is inactive;
- above EFD3, the time to operate is constant and equal to TIME3; and
- if EFD goes below EFD1 at any time before the device has timed-out, the timer resets.

2.10.5 Load Modeling

Several studies, [15, 29], have shown the critical effect of load representation in voltage stability studies and, therefore, the need to find more accurate load models than those traditionally used. Given a power system topology, the behaviour of a system following a disturbance, or the possibility of voltage collapse occurring, depends to a great extent on how the loads are represented.

Loads can be classified into different groups that are generally represented as an aggregated model. The main classifications are as static and dynamic models. As a static load model is not dependent on time, it describes the relationship of the active and reactive power at any time to the voltage and/or frequency at the same instant of time. The characteristics of load with respect to frequency are not critical for the phenomena of voltage stability but those with respect to voltage are. On the other hand, a dynamic load model expresses this active/reactive power relationship at any instant of time as a function of the voltage and/or frequency at a past instant of time, usually including the present moment. Static load models have been used for a long time for both purposes, i.e., to represent static load components, such as resistive and lighting loads, and also to approximate dynamic components. This approximation may be sufficient in some of the cases but for the fact that load representation has critical effects in voltage stability studies. This situation may become worse due to the traditional static load models being replaced with dynamic ones.

The modeling of load is complicated because a typical load bus represented in a stability analysis is composed of a large number of devices, such as fluorescent and incandescent lamps, refrigerators, heaters, compressors, motors and furnaces, etc. The exact composition of load is difficult to estimate. Also, its composition changes depending on many factors, including time, weather conditions and the state of the economy. An example of the composite load model representation used in this dissertation is shown in Fig. 2.6.

Common static load models for active and reactive power are expressed in polynomial or exponential forms and can include, a frequency dependence term. In this book, we use the exponential form to represent static loads as:

$$P(V) = P_0 \left(\frac{V}{V_0} \right)^a \tag{2.14}$$

$$Q(V) = Q_0 \left(\frac{V}{V_0} \right)^b \tag{2.15}$$

where P and Q are active and reactive components of load, respectively, when the bus voltage magnitude is V. The subscript 0 identifies the values of the respective variables at the initial operating condition. The parameters of this model are the exponents a and b. With these exponents equal to 0, 1 or 2, the model represents the constant power, constant current or constant impedance characteristics of load components, respectively.

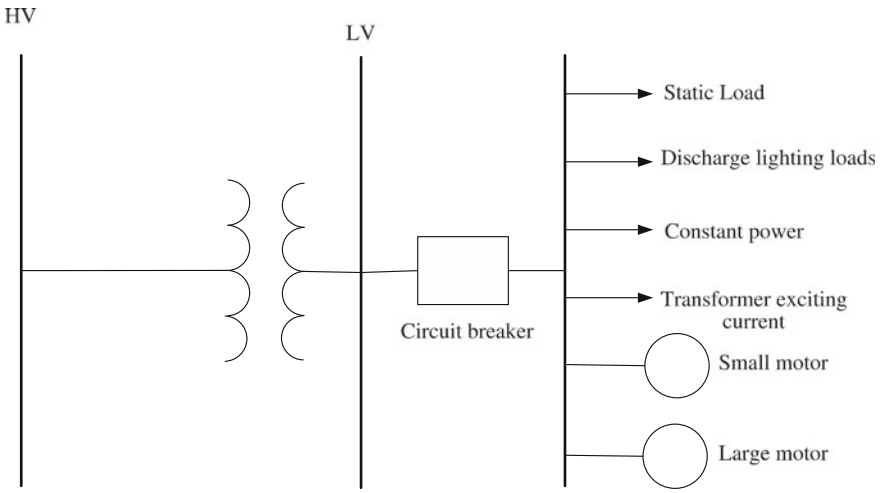

Fig. 2.6 Example of mixed load

2.10.6 Modeling of Induction Motors

A large amount of power consumption is by induction motors (IMs) in residential, commercial and industrial areas, commonly for the compressor loads of air conditioning and refrigeration in residential and commercial areas [18]. These loads require nearly constant torque at all speeds and are the most demanding from a stability viewpoint. On the other hand, pumps, fans and compressors account for more than half of industrial motor use. Typically, motors consume 60 to 70 % of the total power system energy and their dynamics are important for voltage stability and long-term stability studies. Therefore, the dynamics attributed to motors are usually the most significant aspects of the dynamic characteristics of system loads.

For modeling of induction motor in power system stability studies, the transients in stator voltage relations can be neglected [15], which corresponds to ignoring the DC components in stator transient currents, thereby permitting representation of only the fundamental frequency components. The transient model of a squirrel-cage induction motor is described by the following DAEs written in a synchronously-rotating reference frame [15]:

$$(v_{ds_i} + jv_{qs_i}) = (R_{s_i} + jX_i')(i_{ds_i} + ji_{qs_i}) + j(e'_{qr_i} - je'_{dr_i}), \tag{2.16}$$

$$\dot{s} = \frac{1}{2H_{m_i}}\left[T_e - T_L\right], \tag{2.17}$$

$$T'_{do_i}\dot{e}'_{qr_i} = -e'_{qr_i} + (X_i - X_i')i_{ds_i} - T'_{do}s\omega_s e'_{dr}, \tag{2.18}$$

$$T'_{do}\dot{e}'_{dr_i} = -e'_{dr_i} - (X_i - X_i')i_{qr_i} + T'_{do_i}s\omega_s e'_{qr_i}, \tag{2.19}$$

where for $i = 1, \ldots, p$, p is the number of induction motor, $X'_i = X_{s_i} + X_{m_i} X_{r_i} / (X_{m_i} + X_{r_i})$ the transient reactance, $X_i = X_{s_i} + X_{m_i}$ the rotor open-circuit reactance, $T'_{do_i} = (L_{r_i} + L_{m_i})/R_{r_i}$ the transient open-circuit time constant, $T_{e_i} = e'_{qr_i} i_{qs_i} + e'_{dr_i} i_{ds_i}$ the electrical torque, s_i the slip, e'_{dr_i} the direct-axis transient emf, e'_{qr_i} the quadrature-axis transient emf, T_{L_i} the load torque, X_{s_i} the stator reactance, X_{m_i} the magnetising reactance, H_{m_i} the inertia constant of the motor, i_{ds_i} and i_{qs_i} the d- and q-axis components of the stator current, respectively.

There are two ways to obtain aggregation in load models. One is to survey the customer loads in a detailed load model, including the relevant parts of the network, and carry out system reduction. Then, a simple load model can be chosen so that it has similar load characteristics to the detailed load model. Another approach is to choose a load model structure and identify its parameters from measurements.

2.10.7 Modeling of On-Load Tap Changers

Load tap-changing transformers do not correspond to a load component but, seen from a transmission system viewpoint, they may be considered as part of the load. After a disturbance, they restore the sub-transmission and distribution voltages to their pre-disturbance values, but they also affect the status of the voltage-sensitive loads. The restoration of the voltage and, consequently, the increase in these loads may lead the system to voltage instability and collapse. The restoration process takes several minutes. A tap changer is governed by its step size, time constant, reference voltage and deadband. In this model, a tap changing takes place (after some built-in time delay) if the load voltage, V_{rms}, falls outside of a voltage range of $[Vref - D - \varepsilon, Vref + D + \varepsilon]$. The dynamic model of an OLTC is given by:

$$n_{k+1} = n_{k+d}(V_{ref} - V), \tag{2.20}$$

where n_{k+1} and n_k are the turns-ratios before and after a tap change, respectively, and ε, D and d are the hysteresis band, dead-band and step size of the tap, respectively.

2.10.8 Modeling of Wind Generators

The generation of electricity using wind power has received considerable attention world-wide in recent years. With the increasing penetration of wind-derived power in interconnected power systems, it has become necessary to model complete wind energy systems in order to study their impact, and also wind plant controls. Wind energy conversion systems comprise mechanical and electrical equipment and their controls. Modeling these systems for power system stability studies requires careful

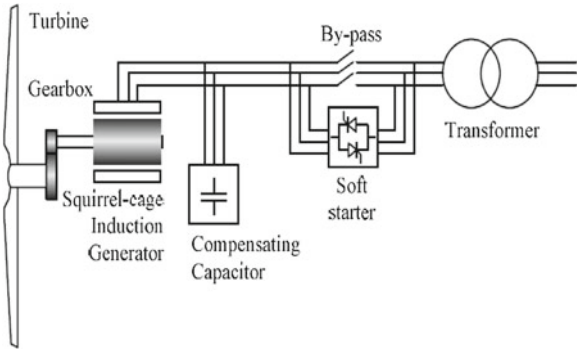

Fig. 2.7 System structure of wind turbine with directly connected squirrel-cage induction generator (source [31])

analysis of the equipment and controls to determine the characteristics that are important in the time frame and bandwidth of such studies.

The response of a wind farm or, alternatively, a model of a wind farm, is very dependent on the type of equipment used. The four concepts of operation of currently used grid-connected wind turbines (WTs) are: constant speed; limited variable speed; variable-speed with partial-scale frequency converter; and variable-speed with full-scale frequency converter [30]. At the moment, the majority of installed WTs are of the fixed-speed types, with SCIGs, known as the 'Danish concept' while, from a market perspective, the dominating technology WTs with doubly-fed induction generators (DFIGs). This book, however, focusses on the fixed-speed wind turbine (FSWT) technology.

FSWTs dominated the first ten years of WT development during the 1990. Operation at constant speed means that, regardless of the wind speed, the WT's rotor speed is fixed and is determined by the frequency of the grid, the gear ratio and the generator design. Usually, a FSWT is equipped with a SCIG connected to the grid, and a soft starter and capacitor bank for reducing the reactive power consumption. It is designed to achieve maximum efficiency at a particular wind speed. Although wound rotor synchronous generators have also been applied, at present, the most common generator is the induction generator (IG).

The schematic structure of a FSWT with a SCIG is depicted in Fig. 2.7. It is the simplest type of WT technology and has a turbine that converts the kinetic energy of wind into mechanical energy. The generator then transforms the mechanical energy into electrical energy and then delivers the energy directly to the grid. It needs to be noted that the rotational speed of the generator, depending on the number of poles, is relatively high (in the order of 1,000–1,500 rpm for a 50 Hz system frequency). Such a rotational speed is too high for the turbine in terms of turbine efficiency and mechanical stress. For this reason, a gear box is used to transform the rotational speed. The fixed-speed induction generator (FSIG) technology operates by drawing reactive power from the external grid via the stator to flux the rotor circuits. This results

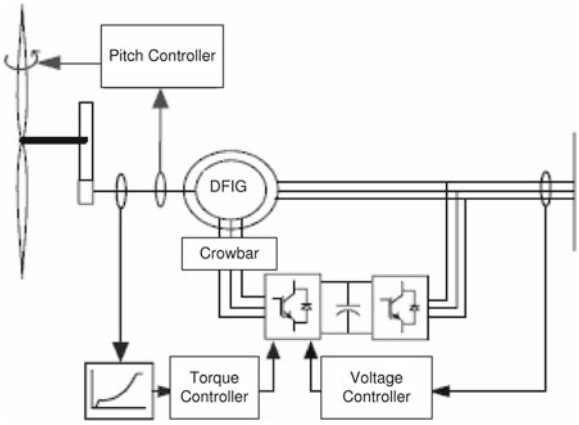

Fig. 2.8 Schematic diagram of variable-speed doubly-fed induction generator (source [32])

in the unit demonstrating a low full-load power factor. Switched capacitor banks or power electronically-controlled reactive power compensation devices (SVCs or STATCOMs) are installed to compensate for the reactive power consumed in order to reduce the intake of reactive power from the grid, hence reducing transmission losses and, in some instances, improving grid stability. The main concern for utilising a FSIG in wind generation is its absorption of excessive reactive power from the power system to magnetise the generator rotor circuit during voltage sag conditions arising from switching-in or system short-circuit fault events. These effects are more pronounced in a weak power system where reactive power reserves are scarce.

The schematic diagram of a variable-speed wind turbine (VSWT) is shown in Fig. 2.8. In this concept, a gear-box is also used. These types of WTs have back-to-back voltage-source converters (VSCs) for feeding the rotor windings and a pitch angle control to limit the power extracted in high wind speed conditions. No compensation capacitors are used.

A power collection and transmission system is required in a wind farm to connect the WTs arrays with the other components of the farm and to transmit the generated power to either distribution or transmission networks depending on the farm's capacity and voltage level [33]. The most common configuration is one in which each turbine unit has a transformer connected to it. However, in some configurations, two or three turbine units are connected together to one transformer. The output power of the transforms is carried by medium-voltage underground cables to overhead or underground collection lines that transmit the power to the wind farm sub-station. Here, the primary transformer steps up the voltage to the required voltage level of the grid.

Wind power has evolved rapidly over the last two decades with regard to the WT power ratings and, consequently, the rotor diameters of WTs. In the past few years, a different type of development has taken place: instead of a continuous increase in WT rated power, the WT manufacturers have focussed on developing WTs that are

more reliable, grid code-compliant and suitable for different installation environments–onshore and offshore. Recently, the commercial offer from the wind industry with the majority of WTs has been rated at around 2–3 MW.

As wind farms become a larger part of the total generation of power systems worldwide, issues related to integration, stability effects and voltage impacts become increasingly important. Adequate load flow and dynamic simulation models (encompassing all significant air-dynamical, mechanical and electrical factors) are necessary to evaluate the impact of wind farms on power systems.

2.10.9 Load Flow Representation

Usually, a wind farm comprises a large number of individual turbine units that are interconnected in a radial or parallel arrangement. When studying the impact of a wind farm on a system, it is reasonable to construct an equivalent of the wind farm with a reduced number of aggregated units connected to the network. Such an aggregated representation is advantageous since it saves the user time and effort in modeling the wind farm. The program available from Siemens PTI allows the user to model a wind farm in PSS/E by merging groups of individual identical units into one or more equivalent machines. These equivalent machines are placed, along with their step-up transformers, at collector buses designated by the user.

The real power output of a WT unit is a function of the wind speed felt by the turbine blades and the site-dependent air density which is related by a so-called power curve. The program mentioned above has the capability to either calculate the MW output based on a given wind speed or, as is more reasonable for system studies, to allow the user to directly dispatch the individual or equivalent units. The reactive power injection or consumption of a WT unit is determined by its dispatch and the AC voltage or power factor control. Based on its control strategy, the program calculates the reactive output and determines the amount of additional shunt capacitors required to be added to provide the desired power factor. In general, the wind farm is represented as a PQ bus in a load-flow study.

The following equations are used to estimate the reactive power output from induction generator [34]:

$$K_1 = X_r + X_m,\ Ax^2 + xB + C = 0, \tag{2.21}$$

where $x = \frac{r_r}{s}, A = P(r_s^2 + K_3^2) - V^2 r_s, B = 2P(r_s K_2 + K_3 K_4) - V^2(K_2 + K_1 + K_3)$, $C = P(K_2^2 + K_4^2) - V^2 K_1 K_4, K_2 = -X_s K_1 - X_r X_m, K_3 = X_s + X_m, K_4 = r_s K_1$, and $P = \frac{V^2(xT_1 + K_1 T_2)}{T_3}$. Then, the reactive power of the IG is given by

$$Q_g = -\frac{V^2(K_1 T_1 - x_1 T_2)}{T_3}, \tag{2.22}$$

where $T_1 = xR_s - X_s K_1 - X_r X_m, T_2 = x(X_m + X_s) + r_s K_1, T_3 = T_1^2 + T_2^2$.

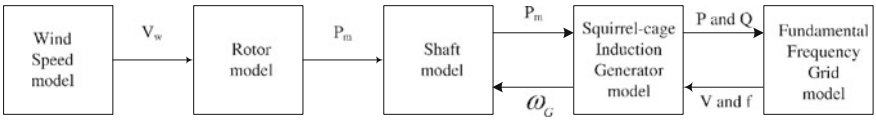

Fig. 2.9 General structure of constant-speed wind turbine model

2.10.10 Dynamic Model of Wind Generators

This book uses a model of the induction generator written in appropriate d-q reference frame to facilitate investigation of control strategies. Figure 2.9 depicts the general structure of a model of a constant-speed wind turbine. The most important components of a constant speed wind turbine are rotor, drive train and the generator, combined with a wind speed model.

2.10.11 Rotor Model

WTs are the main components of wind farms. They are usually mounted on towers to capture the most kinetic energy. Because the wind speed increases with height, taller towers enable turbines to capture more energy and generate more electricity. The three bladed rotor, consisting of the blades and a hub, is the most important and most visible part of a WT. It is through the rotor that the energy of the wind is transformed into mechanical energy that turns the main shaft of a WT.

The rotor of a WT, with radius R_i, converts energy from the wind to the rotor shaft, rotating at the speed of ω_{m_i}. The power from the wind depends on the wind speed, V_{w_i}, the air density, ρ_i, and the swept area, A_{wt_i}. From the available power in the swept area, the power on the rotor is given based on the power coefficient, $c_{p_i}(\lambda_i, \theta_i)$, which depends on the pitch angle of the blade, θ_i, and the ratio between the speed of the blade tip and the wind speed, denoted as the tip-speed ratio, $\lambda_i = \frac{\omega_{m_i} R_i}{V_{w_i}}$. The aerodynamic torque applied to the rotor for the *ith* turbine by the effective wind speed passing through the rotor is given as [30]:

$$T_{ae_i} = \frac{\rho_i}{2\omega_{m_i}} A_{wt_i} c_{p_i}(\lambda_i, \theta_i) V_{w_i}^3, \tag{2.23}$$

where c_{p_i} is approximated by the following relationship [35]:

$$c_{p_i} = (0.44 - 0.0167\theta_i) \sin\left[\frac{\pi(\lambda_i - 3)}{15 - 0.3\theta_i}\right] - 0.00184(\lambda_i - 3)\theta_i,$$

where $i = 1, \cdots, n$ and n is the number of WTs.

A controller equipped with a WT starts up the machine at wind speeds of about 8–16 miles per hour (mph) and shuts it off at about 55 mph. Turbines do not operate at wind speeds above about 55 mph because they might be damaged. The radius of a 2 MW wind turbine is about 80m, the typical value of air density is 1.225 kg/m^3, c_p is in the range of 0.52–0.55, towers range from 60 to 90 m (200 to 300 feet) tall and the blades rotate at 10–22 revolutions per minute.

Equation 2.23 shows that aerodynamic efficiency is influenced by variation in the blade's pitch angle. Regulating the rotor blades provides an effective means of regulating or limiting the turbine power during high wind speeds or abnormal conditions. A pitch controlled turbine performs power reduction by rotating each blade about its axis in the direction of the angle of attack. In comparison with the passive stall, the pitch control provides greater energy capture at the rated wind speed and above. The aerodynamic braking facility of the pitch control can reduce extreme loads on a turbine and also limit its power input so as to control possible over-speed of the machine if the loading of the turbine-generator system is lost, for instance, because of a power system fault. On a pitch-controlled WT, electronic controllers check the power output of the turbine several times per second. When the power output becomes too high, a message is sent to the blade-pitch mechanism which immediately turns the rotor blades slightly in an attempt to restore this output to an acceptable value. In this work, the pitch-rate limit is set to the typical value of 12 deg s^{-1}.

2.10.12 Shaft Model

A two-mass drive train model of a WT generator system (WTGS) is commonly used as drive train modeling can satisfactorily reproduce the dynamic characteristics of a WTGS because the low-speed shaft of a WT is relatively soft [36]. Therefore, although, it is essential to incorporate a shaft representation into the constant-speed wind turbine model, only a low-speed shaft is included. The gearbox and high-speed shaft are assumed to be infinitely stiff. The resonance frequencies associated with gearboxes and high-speed shafts usually lie outside the frequency bandwidth of interest [37]. Therefore, we use a two-mass representation of the drive train.

The drive train attached to the WT converts the aerodynamic torque, T_{ae_i}, on the rotor into the torque on the low-speed shaft, which is scaled down through the gear-box to the torque on the high-speed shaft. The first mass term stands for the blades, hub and low-speed shaft and the second for the high-speed shaft with inertia constants, H_{m_i} and H_{G_i}, respectively. The shafts are interconnected by a gear ratio, N_{g_i}, combined with torsion stiffness, K_{s_i}, and torsion damping, D_{m_i} and D_{G_i}, resulting in the torsion angle, γ_i. The normal grid frequency is f. The dynamics of the shaft are represented as in [30]:

$$\dot{\omega}_{m_i} = \frac{1}{2H_{m_i}} \left[T_{ae_i} - K_{s_i}\gamma_i - D_{m_i}\omega_{m_i} \right], \tag{2.24}$$

$$\dot{\omega}_{G_i} = \frac{1}{2H_{G_i}} \left[K_{s_i} \gamma_i - T_{e_i} - D_{G_i} \omega_{G_i} \right], \tag{2.25}$$

$$\dot{\gamma}_i = 2\pi f (\omega_{m_i} - \frac{1}{N_{g_i}} \omega_{G_i}). \tag{2.26}$$

The generator receives the mechanical power from the gear-box through the stiff shaft. The relationship between the mechanical torque and the torsional angle is given by:

$$T_{mi} = K_{s_i} \gamma_i. \tag{2.27}$$

The gear-box connects the low-speed shaft to the high-speed shaft and increases the rotational speeds from about 30 to 60 rotations per minute (rpm) to about 1,000–1,800 rpm, which is the rotational speed required by most generators to produce electricity.

2.10.13 Induction Generator Model

An IG can be represented in different ways, depending on the level of detail characterised mainly by the number of phenomena, such as stator and rotor flux dynamics, magnetic saturation, skin effects and mechanical dynamics included. Although, a very detailed model which includes all these dynamics is a possibility, it may not be beneficial for stability studies because it increases the complexity of the model and requires time-consuming simulations. More importantly, not all of these dynamics are shown to have significant influence in stability studies.

A comparison of different induction generator models can be found in [30]. Accordingly, as the inclusion of iron losses in a model is a complicated task, its influence for stability studies is neglected. The main flux saturation is only of importance when the flux level is higher than the nominal level. Hence, this effect can be neglected for most operating conditions. The skin effect should only be taken into account for a large-slip operating condition which is not the case for a FSWT.

Another constraint of including dynamics in a model is the availability of relevant data. Typically, saturation and skin effect data are not provided by manufacturers. Therefore, in general, it is impractical to use them in WT applications. For the representation of FSIG models in power system stability studies [38], the stator flux transients can be neglected in the voltage relations.

All of these arguments lead to the conclusion that rotor dynamics are only the major factors required to be considered in an IG model for a voltage stability analysis. Representation of the third-order model of an IG offers a compatibility with the network model and provides more efficient simulation time. The main drawbacks of the third-order model is its inability to predict peak transient current and, to some extent, its less accurate estimation of speed. However, at a relatively high inertia, the third-order model is sufficiently accurate.

The transient model of a SCIG is described by the following DAEs [30, 34]:

$$\dot{s}_i = \frac{1}{2H_{G_i}}\left[T_{m_i} - T_{e_i}\right], \tag{2.28}$$

$$\dot{E}'_{qr_i} = -\frac{1}{T'_{o_i}}\left[E'_{qr_i} - (X_i - X'_i)i_{ds_i}\right] - s_i\omega_s E'_{dr_i}, \tag{2.29}$$

$$\dot{E}'_{dr_i} = -\frac{1}{T'_{o_i}}\left[E'_{dr_i} + (X_i - X'_i)i_{qs_i}\right] + s_i\omega_s E'_{qr_i}, \tag{2.30}$$

$$V_{ds_i} = R_{s_i}i_{ds_i} - X'_i i_{qs_i} + E'_{dr_i}, \tag{2.31}$$

$$V_{qs_i} = R_{s_i}i_{ds_i} + X'_i i_{qs_i} + E'_{qr_i}, \tag{2.32}$$

$$v_{t_i} = \sqrt{V^2_{ds_i} + V^2_{qs_i}}, \tag{2.33}$$

where $X'_i = X_{s_i} + X_{m_i}X_{r_i}/(X_{m_i} + X_{r_i})$ is the transient reactance, $X_i = X_{s_i} + X_{m_i}$ the rotor open-circuit reactance, $T'_{o_i} = (L_{r_i} + L_{m_i})/R_{r_i}$ the transient open-circuit time constant, v_{t_i} the terminal voltage of the IG, s_i the slip, E'_{dr_i} the direct-axis transient voltages, E'_{qr_i} the quadrature-axis transient voltages, V_{ds_i} the d-axis stator voltage, V_{qs_i} the q-axis stator voltage, T_{m_i} the mechanical torque, $T_{e_i} = E_{dr_i}i_{ds_i} + E_{qr_i}i_{qs_i}$, the electrical torque, X_{s_i} the stator reactance, X_{r_i} is the rotor reactance, X_{m_i} the magnetising reactance, R_{s_i} the stator resistance, R_{r_i} the rotor resistance, H_{G_i} the inertia constant of the IG, and i_{ds_i} and i_{qs_i} the d- and q-axis components of the stator current, given by:

$$I_{di} = \sum_{j=1}^{n}\left[E'_{drj}(G_{ij}\cos\delta_{ji} - B_{ij}\sin\delta_{ji}) + E'_{qrj}(G_{ij}\sin\delta_{ji} + B_{ij}\cos\delta_{ji})\right], \tag{2.34}$$

$$I_{qi} = \sum_{j=1}^{n}\left[E'_{drj}(G_{ij}sin\delta_{ji} + B_{ij}cos\delta_{ji}) + E'_{qrj}(G_{ij}cos\delta_{ji} - B_{ij}sin\delta_{ji})\right]. \tag{2.35}$$

2.10.14 Modeling of DFIG

The equations that describe a SCIG are identical to those of the DFIG except that the rotor is short-circuited. The converter for DFIGs [30] used in this book consists of two VSCs connected back-to-back. This enables variable-speed operation of the WTs by using a decoupling control scheme which controls the active and reactive components of the current separately. The modeling of IGs for power-flow and dynamic analyses is discussed in [30, 34].

The DC-link dynamic of a DFIG is given by:

$$C_i v_{dc_i} \dot{v}_{dc_i} = -\frac{v_{dc_i}^2}{R_{loss_i}} - P_{r_i}(t) - P_{g_i}(t) \tag{2.36}$$

where resistor R_{loss_i} represents the total conducting and switching losses of the converter. Also, $P_{r_i}(t)$ is the instantaneous input rotor power, and $P_{g_i}(t)$ is the instantaneous output power of the GSC which are given by:

$$P_{r_i} = v_{rd_i} i_{rd_i} + v_{rq_i} i_{rq_i}, \tag{2.37}$$

$$P_{g_i} = v_{gd_i} i_{gd_i} + v_{gq_i} i_{gq_i}. \tag{2.38}$$

2.10.15 Aggregated Model of Wind Turbine

The development of aggregated models of wind farms is also an important issue because, as the sizes and numbers of turbines on wind farms increase, representing wind farms as individual turbines increases complexity and leads to a time-consuming simulation which is not beneficial for stability studies of large power systems.

For the aggregation of WTs, the models of several identical WTs (even in the incoming wind) are combined in a single turbine model with a higher rating. The parameters are obtained by preserving the electrical and mechanical parameters of each unit, and by increasing the nominal power to the equivalent of the involved turbines in the aggregation process [39].

This aggregated model reduces computation and simulation times in comparison with those of a detailed model with different representations of tens or hundreds of turbines and their interconnections. However, the aggregated model requires specific care in choosing what to aggregate in order to be as close to reality as possible. In addition, this type of modeling is very difficult for WTs without a parallel distribution (i.e., in the form of an array which is the most common distribution for offshore, but not for onshore, wind farms).

2.10.16 Modeling of PV Unit

As shown in Fig. 2.10, PV plants have mainly two parts (a) solar conversion and (b) electrical interface with the electrical network (a power electronic converter). A PV array is connected to the grid through a DC–DC converter and a DC-AC inverter. A DC–DC converter enables the transfer of maximum power from the solar module to the inverter. The PV array as shown in Fig. 2.11 is described by its current-voltage characteristics function [40, 41]:

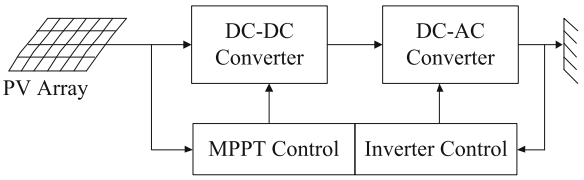

Fig. 2.10 Block Diagram of a PV System

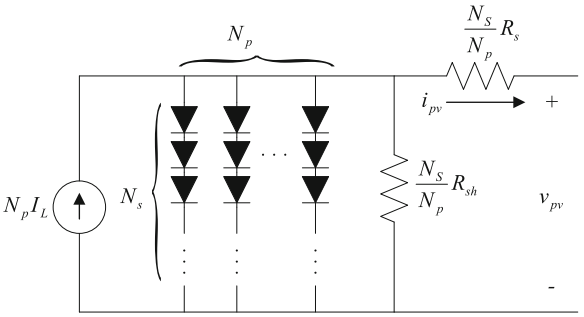

Fig. 2.11 Equivalent circuit of a PV array

$$i_{\mathrm{pv}_i} = N_{\mathrm{p}_i} I_{\mathrm{L}_i} - N_{\mathrm{p}_i} I_{\mathrm{s}_i} \left[\exp\left[\alpha_{p_i} \left(\frac{v_{\mathrm{pv}_i}}{N_{\mathrm{s}_i}} + \frac{R_{\mathrm{s}_i} i_{\mathrm{pv}_i}}{N_{\mathrm{p}_i}} \right) \right] - 1 \right] - \frac{N_{\mathrm{p}_i}}{R_{\mathrm{sh}_i}} \left(\frac{v_{\mathrm{pv}_i}}{N_{\mathrm{s}_i}} + \frac{R_{\mathrm{s}_i} i_{\mathrm{pv}_i}}{N_{\mathrm{p}_i}} \right), \tag{2.39}$$

where I_{L_i} is the light-generated current, I_{s_i} is the reverse saturation current, chosen as 9×10^{-11} A, N_{s_i} is the number of cells in series and N_{p_i} is the number of modules in parallel, R_{s_i} and R_{sh_i} are the series and shunt resistances of the array respectively, i_{pv_i} is the current flowing through the array, and v_{pv_i} is the output voltage of the array. The constant α_{p_i} in Eq. (9.1) is given by

$$\alpha_{p_i} = \frac{q_i}{A_i k_i T_{\mathrm{r}_i}} \tag{2.40}$$

where $k_i = 1.3807 \times 10^{-23} JK^{-1}$ is the Boltzmann constant, $q_i = 1.6022 \times 10^{-19}$ C is the charge of the electron, A_i is the p–n junction ideality factor with a value between 1 and 5, and T_{r_i} is the cell reference temperature. The schematic of a grid-connected PV system consisting of switching elements is shown in Fig. 2.12 [42, 43]. A nonlinear model of the three-phase grid connected PV system shown in Fig. 2.12 can be written as [42, 43]:

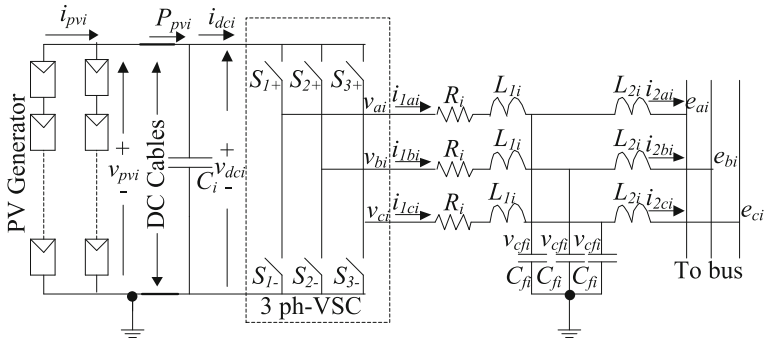

Fig. 2.12 PV system connected to the grid

$$\begin{aligned}
\dot{i}_{1\mathrm{a}_i} &= -\frac{R_i}{L_{1_i}} i_{1\mathrm{a}_i} - \frac{1}{L_{1_i}} e_{\mathrm{a}_i} + \frac{v_{\mathrm{pv}_i}}{3L_{1_i}} (2K_{\mathrm{a}_i} - K_{\mathrm{b}_i} - K_{\mathrm{c}_i}) \\
\dot{i}_{1\mathrm{b}_i} &= -\frac{R_i}{L_{1_i}} i_{1\mathrm{b}_i} - \frac{1}{L_{1_i}} e_{\mathrm{b}_i} + \frac{v_{\mathrm{pv}_i}}{3L_{1_i}} (-K_{\mathrm{a}_i} + 2K_{\mathrm{b}_i} - K_{\mathrm{c}_i}) \\
\dot{i}_{1\mathrm{c}_i} &= -\frac{R_i}{L_{1_i}} i_{1\mathrm{c}_i} - \frac{1}{L_{1_i}} e_{\mathrm{c}_i} + \frac{v_{\mathrm{pv}_i}}{3L_{1_i}} (-K_{\mathrm{a}_i} - K_{\mathrm{b}_i} + 2K_{\mathrm{c}_i})
\end{aligned} \tag{2.41}$$

$$\begin{aligned}
\dot{v}_{\mathrm{cfa}_i} &= \frac{1}{C_{\mathrm{f}_i}} \left(i_{1\mathrm{a}_i} - i_{2\mathrm{a}_i}\right), \ \dot{v}_{\mathrm{cfb}_i} = \frac{1}{C_{\mathrm{f}_i}} \left(i_{1\mathrm{b}_i} - i_{2\mathrm{b}_i}\right) \\
\dot{v}_{\mathrm{cfc}_i} &= \frac{1}{C_{\mathrm{f}_i}} \left(i_{1\mathrm{c}_i} - i_{2\mathrm{c}_i}\right), \ \dot{i}_{2\mathrm{a}_i} = \frac{1}{L_{2_i}} \left(v_{\mathrm{cfa}_i} - e_{\mathrm{a}_i}\right) \\
\dot{i}_{2\mathrm{b}_i} &= \frac{1}{L_{2_i}} \left(v_{\mathrm{cfb}_i} - e_{\mathrm{b}_i}\right), \ \dot{i}_{2\mathrm{c}_i} = \frac{1}{L_{2_i}} \left(v_{\mathrm{cfc}_i} - e_{\mathrm{c}_i}\right)
\end{aligned} \tag{2.42}$$

where K_{a_i}, K_{b_i}, and K_{c_i} are the binary input switching signals. By applying KCL at the node where the DC link is connected, we get

$$\dot{v}_{\mathrm{pv}_i} = \tfrac{1}{C_i} \left(i_{\mathrm{pv}_i} - i_{\mathrm{dc}_i}\right). \tag{2.43}$$

The input current of the inverter i_{dc_i} can be written as [43]

$$i_{\mathrm{dc}_i} = i_{\mathrm{a}_i} K_{\mathrm{a}_i} + i_{\mathrm{b}_i} K_{\mathrm{b}_i} + i_{\mathrm{c}_i} K_{\mathrm{c}_i}. \tag{2.44}$$

Now Eq. (2.43) can be rewritten as:

$$\dot{v}_{\mathrm{pv}_i} = \tfrac{1}{C_i} i_{\mathrm{pv}_i} - \tfrac{1}{C_i} \left(i_{\mathrm{a}_i} K_{\mathrm{a}_i} + i_{\mathrm{b}_i} K_{\mathrm{b}_i} + i_{\mathrm{c}_i} K_{\mathrm{c}_i}\right). \tag{2.45}$$

Equations (2.41) and (2.45) can be transformed into dq frame using the angular frequency ω_i of the grid as:

$$\begin{aligned}
L_{1_i}\dot{i}_{1\mathrm{d}_i} &= -R_i i_{1\mathrm{d}_i} + \omega_i L_{1_i} i_{1\mathrm{q}_i} - v_{\mathrm{cfd}_i} + K_{\mathrm{d}_i} v_{\mathrm{pv}_i} \\
L_{1_i}\dot{i}_{1\mathrm{q}_i} &= -R_i i_{1\mathrm{q}_i} - \omega_i L_{1_i} i_{1\mathrm{d}_i} - v_{\mathrm{cfq}_i} + K_{\mathrm{q}_i} v_{\mathrm{pv}_i} \\
L_{2_i}\dot{i}_{2\mathrm{d}_i} &= +\omega_i L_{2_i} i_{2\mathrm{q}_i} + v_{\mathrm{cfd}_i} - E_{\mathrm{d}_i} \\
L_{2_i}\dot{i}_{2\mathrm{q}_i} &= -\omega L_2 i_{2\mathrm{d}} + v_{\mathrm{cfq}} - E_{\mathrm{q}} \\
C_{\mathrm{f}_i}\dot{v}_{\mathrm{cfd}_i} &= \omega_i C_{\mathrm{f}_i} v_{\mathrm{cfq}_i} + C_{\mathrm{f}_i}\left(i_{1\mathrm{d}_i} - i_{2\mathrm{d}_i}\right) \\
C_{\mathrm{f}_i}\dot{v}_{\mathrm{cfq}_i} &= -\omega_i C_{\mathrm{f}_i} v_{\mathrm{cfd}_i} + C_{\mathrm{f}_i}\left(i_{1\mathrm{q}_i} - i_{2\mathrm{q}_i}\right) \\
C_i\dot{v}_{\mathrm{pv}_i} &= i_{\mathrm{pv}_i} - i_{1\mathrm{d}_i} K_{\mathrm{d}_i} - i_{1\mathrm{q}_i} K_{\mathrm{q}_i}
\end{aligned} \tag{2.46}$$

The synchronization scheme for $abc \rightarrow dq$ transformation is chosen such that the q-axis of the dq frame is aligned with the grid voltage vector, $E_{\mathrm{q}_i} = 0$, and the real and reactive power delivered to the grid can be written as $P_i = \frac{3}{2} E_{\mathrm{d}_i} I_{\mathrm{d}_i}$ and $Q_i = -\frac{3}{2} E_{\mathrm{d}_i} I_{\mathrm{q}_i}$.

2.10.17 Modeling of FACTS Devices

In general, FACTS devices can be utilised to increase the transmission capacity, the stability margin and dynamic behaviour and serve to ensure improved power quality. Their main capabilities are reactive power compensation, voltage control and power-flow control. Due to their controllable power electronics, FACTS devices always provide fast controllability in comparison with that of conventional devices, such as switched compensation or phase shifting transformers. Different control options provide high flexibility and lead to multi-functional devices.

Several kinds of FACTS devices have been developed and there are several years of documented evidence of their use in practice and research. Some of them, such as the thyristor based SVC, are widely applied technology; others, like the VSC-based STATCOMs or the VSC high voltage DC (HVDC) are being used in a growing number of installations worldwide. The most versatile FACTS devices, such as the unified power-flow controller (UFPC) are still confined primarily to research and development applications. In this book, we mainly use a STATCOM and, in few cases, SVC and thyristor-controlled switched capacitors (TCSCs).

2.10.18 STATCOM Model

The concept of the STATCOM was proposed by Gyugyi in 1976 [44]. A STATCOM is a shunt FACTS device which is mostly employed for controlling the voltage at

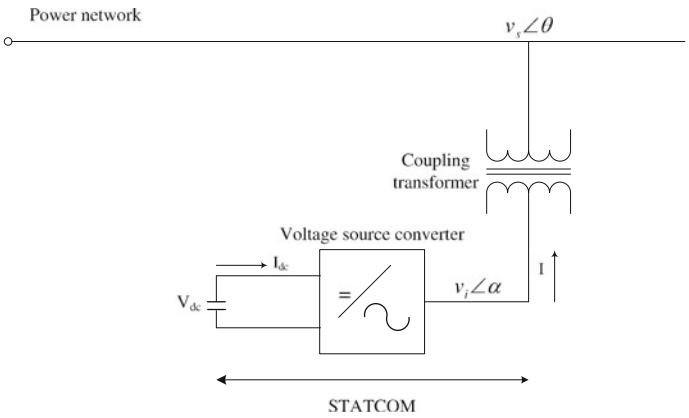

Fig. 2.13 Schematic diagram of VSC-based STATCOM

the point of connection to the network, as shown in Fig 2.13. In general, a STATCOM system consists of three main parts: a VSC; a coupling reactor or a step-up transformer; and a controller. The magnitude and phase of VSC's output voltage, V_i, can be regulated through the turn-on/turn-off of the VSC switches so that the VSC output current, I, can be controlled. Here, I is equal to the sum of V_i minus the voltage at an AC point of common coupling (PCC), V_s, divided by the impedance of the coupling reactor, X_s. In other words, the capacitive or inductive output currents of a STATCOM can be achieved through regulating the magnitude of V_i to be larger or smaller than the magnitude of V_s. Meanwhile, the phase of V_i is almost in phase with V_s but has a small phase-shift angle to compensate for the converter's internal loss, thereby keeping the system stable. Therefore, I can be controlled inherently and independently of V_s.

By controlling the magnitude and angle of its output voltage, i.e., $V_i\angle\alpha$, the STATCOM is able to control its active and reactive exchanges with the power system and, therefore, control the voltage at the PCC. The real and reactive power expressions are given by:

$$P = \frac{V_i V_s}{X}\sin(\alpha - \theta),$$
$$Q = \frac{V_i(V_i - V_s\cos(\alpha - \theta))}{X}.$$

The direction of the reactive power flow can now be determined by the magnitude of the inverter output voltage. For values of V_i larger than V_s, a STATCOM is in the capacitive mode and injects reactive power into the network while, for V_i values smaller than V_s, it is in the inductive mode and absorbs reactive power from the network. In a typical STATCOM with a capacitor as the DC link, the values of the active and reactive power depend on one another. However, a STATCOM connected

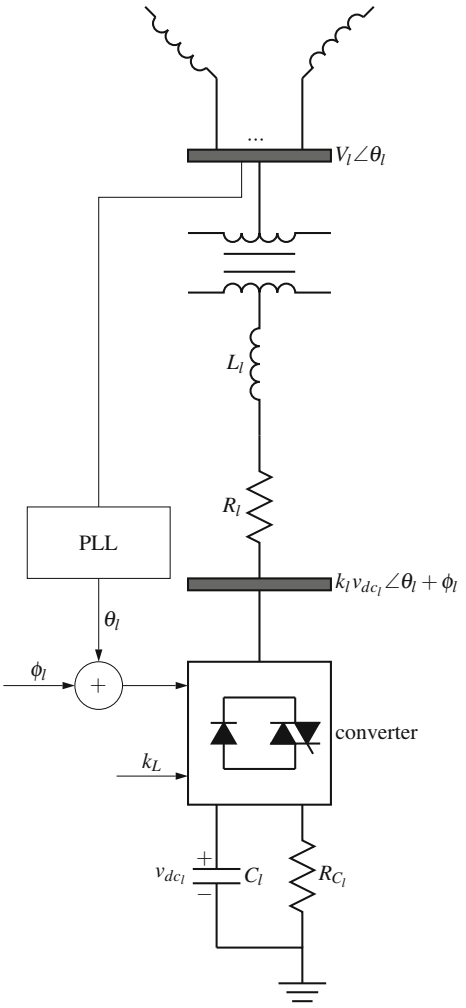

Fig. 2.14 Schematic diagram of STATCOM

to a battery energy storage system (STATCOM/BESS) is capable of controlling the values of both the active and reactive power independently [45].

For the purposes of stability studies, the STATCOM shown in Fig. 2.14 can be modelled as an AC voltage source with controllable magnitude and phase [46]. The dynamics of this voltage source are governed by the charging and discharging of a large (nonideal) capacitor. The capacitor, C_l, and its resistance, R_{C_l}, are shown in Fig. 2.14. The DC voltage across the capacitor is inverted and connected to an external bus via a short transmission line and a transformer bus. Details of various inverter schemes and how a controllable phase and magnitude are achieved are described in [44]. The phase-locked loop (PLL) block in Fig. 2.14 indicates that the phase shift of the inverter wave is adjusted with reference to the external bus voltage.

For the stability analysis we include the transformer and the transmission line (represented by R_l and L_l in Fig. 2.14) in the reduced impedance matrix. This directly interconnects the controllable inverter output with the rest of the system. The capacitor voltage can be adjusted by controlling the phase-angle difference between the line voltage, V_l, and the VSC voltage, E_l, ($E_l = k_l v_{dc_l} \angle \alpha_l$). If the phase angle of the line voltage is taken as a reference, the phase angle of the VSC voltage is the same as the firing angle, α_l, of the VSC. Thus, if the firing angles are slightly advanced, the DC voltage, v_{dc_l}, decreases and the reactive power flows into the STATCOM. Conversely, if the firing angles are slightly delayed, the DC voltage increases and the STATCOM supplies reactive power to the bus. By controlling the firing angle of the VSC, the reactive power can be generated from, or absorbed, by the STATCOM and, thus, voltage regulation can be achieved.The dynamics for l^{th} STATCOM can be described by the following equation:

$$\dot{v}_{dc_l}(t) = -\frac{P_{s_l}}{C_l v_{dc_l}} - \frac{v_{dc_l}}{R_{C_l} C_l}, \tag{2.47}$$

for $l = 1, \ldots, m$ where m is the number of STATCOMs, v_{dc_l} the capacitor voltage, C_l the DC capacitor, R_{C_l} the internal resistance of the capacitor, α_l the bus angle of the STATCOM in the reduced network, and P_{s_l} the power supplied by the system to the STATCOM to charge the capacitor which is given by:

$$\begin{aligned} P_{s_l} = |E_l|^2 G_{ll} + \sum_{\substack{p=1 \\ p \neq l}}^{m} |E_l||E_p| \left[B_{lp} \sin \alpha_{pl} + G_{pl} \cos \alpha_{lp} \right], \\ + \sum_{\substack{j=1 \\ j \neq l}}^{n} |E_l||E'_j| \left[B_{lj} \sin(\delta_j - \alpha_l) + G_{lj} \cos(\delta_j - \alpha_l) \right], \end{aligned} \tag{2.48}$$

where G_{lp} and B_{lp} are the real and imaginary parts of the equivalent transfer impedances between the terminal buses of STATCOMs l and p and G_{lj} and B_{lj} are between the terminal buses of STATCOM l and IG j. The term E'_j denotes both E'_{drj} and E'_{qrj} and $\sin \alpha_{pl} = \sin(\alpha_p - \alpha_l)$.

The terminal voltage of STATCOMs is measured using a transducer with firs-order dynamic:

$$\dot{v}_{tm_l} = -\frac{v_{tm_l}}{T_{m_l}} + K_{m_l} v_{t_l}, \tag{2.49}$$

where v_{tm_l} is the sensor output, v_{t_l} the voltage at the connection point of STATCOM, K_{m_l} the constant and T_{m_l} the time constant of the voltage transducer. For the linear analysis we can assume that we know the equilibrium condition α_0 and control only $\Delta\alpha$ as shown in Fig. 2.15.

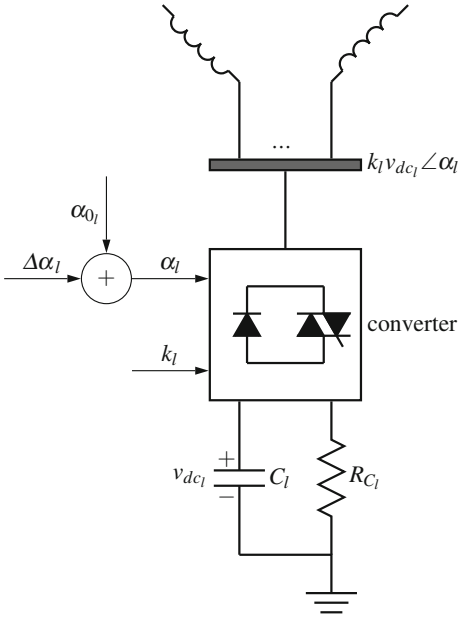

Fig. 2.15 STATCOM (equivalent)

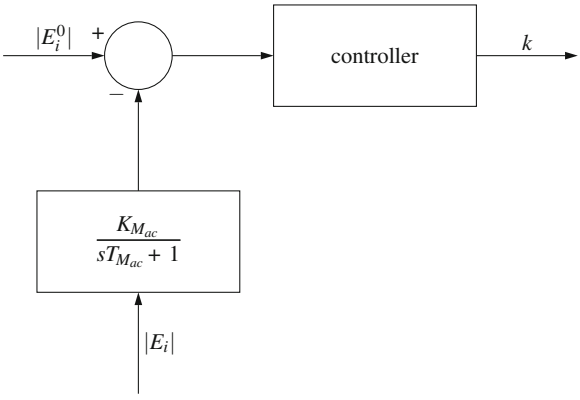

Fig. 2.16 Modulation index (k) control

The indirect conventional controllers for k and α are shown in Figs. 2.16 and 2.17. This gives an idea of the controller structure used by the industry. In this research, we will control Δk and $\Delta\alpha$ for the STATCOM in Fig. 2.15 directly instead of using conventional controllers.

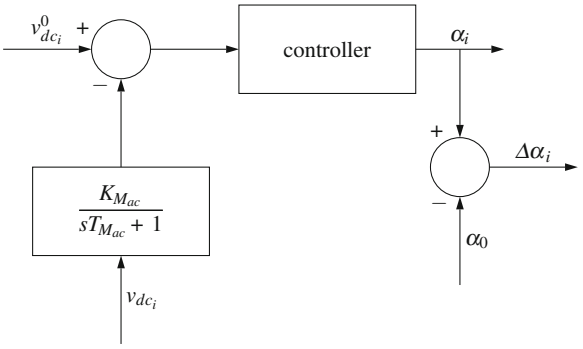

Fig. 2.17 Firing angle (α) control

2.10.19 SVC Modeling

By providing dynamic reactive power, SVC can be used for the purpose of regulating the system voltage, compensating the voltage at a reasonable level, improving the power flow capacity of a transmission line, enhancing the damping of low frequency oscillations as well as inhibiting the sub-synchronous oscillations. SVC is also capable of inhibiting the variation of busbar voltage caused by the fluctuating load, which is favourable for the recovery of transient voltage and the improvement of stabilisation of the system voltage.

For industrial users, it can effectively control the reactive power, improve the power factor, reduce the voltage influence and harmonic interference caused by the nonlinear load, balance the three-phase load, improve the power quality, productive efficiency and the product quality, and reduce the energy consumption. It is widely used in the machine, electric power, metallurgy, electrified railway, mine and wind power generation industries. The overall performance indicators are given below:

- SVC dynamic capacity: 0–400 MVAr;
- control-target bus rated voltage: 6–500 kV;
- total dynamic response time: (reactive power output): $<$15 ms; and
- SVC biggest loss: $<$0.8 %.

The SVC circuit contains the voltage measuring and voltage regulator circuits, outputs of which are fed into the thyristor firing control circuit. Normally, the susceptance of the SVC (B) is varied to maintain the mid-bus voltage, V_m, within its pre-specified tolerance. The supplementary stabilising signal is added to the output of the voltage regulator. The variation of the susceptance (B) can be related through the differential equation:

$$\triangle \dot{B}_l = \left[-\triangle B_l + B_{l0} + K_{c_l} V_{s_l}\right] / T_{c_l}, \tag{2.50}$$

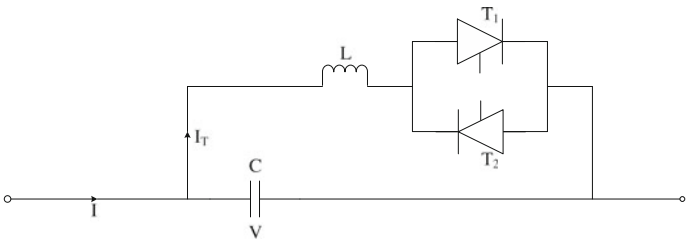

Fig. 2.18 One-line diagram of single-phase TCSC

for $l = 1, \ldots, m$, where m is the number of SVC, K_{cl} and T_{cl} the gain and time constants of the SVC's firing angle control circuit, respectively, and V_{sl} the extra stabilising signal.

2.10.20 Thyristor Controlled Series Capacitor

After the introduction of TCSC in the late 1980s, they have been implemented in several locations around the world. As a controllable series compensation device and with flexible control possibilities, the TCSC has been found to be effective, especially in damping electromechanical and sub-synchronous oscillations. With a properly designed control system, a TCSC can be effectively utilised for enhancing both small signal and transient stabilities of a power system. Therefore, a good understanding of the interaction phenomena between a TCSC and its surrounding network will be necessary in order to design optimal control structures and, at the same time, prevent undesired interactions.

The single-line diagram of a TCSC is shown in Fig. 2.18. The operation of a TCSC involves discrete actions and is periodic in nature, whereby one of its anti-parallel thyristors of the TCSC is turned on during a portion of a half-cycle of the power frequency and is turned-off during the remainder of the cycle. The other anti-parallel thyristor repeats the conduction/non-conduction process during the next half cycle and vice versa. The duration and timing of thyristor conductions are based on the triggering logic and are controlled by the synchronisation system and the higher-level control loops. When a thyristor conducts, a circulating current flows in both the inductor and the capacitor which can either increase or decrease the voltage across the capacitor.

2.10.21 Energy Storage Device

The energy storage system (ESS), as an enabling infrastructure technology, provides ride-through over outages, improves profitability in high-energy applications,

increases system reliability and dynamic stability, improves power quality and enhances transmission capacity of the transmission grid in a high power application [44]. For a high power application, the use of short-term (cycles to seconds) energy storage integrated with a power electronics-based controller, well known as a FACTS controller, could offer the following three distinct advantages:

- provide system damping, while maintaining constant voltage following a disturbance;
- provide additional damping in situations where the dynamic reactive power provided by traditional FACTS controllers with similar ratings is inadequate (alternatively, it could provide the same amount of damping at less cost. The damping of oscillation, by repeatedly interchanging small amounts of real power with the system, would be an excellent ESS application); and
- provide energy to maintain the speed of locally connected induction motors during a power system disturbance (This may prevent a voltage collapse in areas where there is a large concentration of induction motors that would otherwise stall).

While the superconductive magnetic energy storage (SMES) technology overcomes many barriers from a technology perspective, and has been commercially available in some specific sizes, the cost and relative complexity of the overall SMES system still makes it an expensive choice for a short-term ESS [47].

Recent advances in supercapacitor (SCAP) technology with an asymmetrical design have brought much excitement to the industry with the hope of a new and better short-term energy storage solution [48]. SCAP, as one type of electrochemical capacitor, stores electrical energy in the electrical double layer using relatively inexpensive materials, provides energy density thousands of times larger than that of conventional electrolytic capacitors, and has miscellaneous advantages over other high-power energy storage devices: high power density, low cost, reliable and long life cycle, fast and deep charge/discharge capability, wide range of operational temperatures, maintenance-free operation and storage, and environmental safety. These characteristics make SCAP a desirable energy storage element for short-term high-power ESS applications [49].

2.10.22 Network Power-Flow Model

The power balance equations pertaining to generator buses are given by:

$$V_i \cos(\delta_i - \theta_i) I_{q_i} - V_i \sin(\delta_i - \theta_i) I_{d_i} - S_{p_i} = 0, \tag{2.51}$$

$$-V_i \sin(\delta_i - \theta_i) I_{q_i} - V_i \cos(\delta_i - \theta_i) I_{d_i} - S_{q_i} = 0, \tag{2.52}$$

where,

$$S_{p_i} = \sum_{k=1}^{n} V_i V_k \left[G_{ik} \cos(\theta_i - \theta_k) + B_{ik} \sin(\theta_i - \theta_k) \right], \tag{2.53}$$

$$S_{q_i} = \sum_{k=1}^{n} V_i V_k \left[G_{ik} \sin(\theta_i - \theta_k) - B_{ik} \cos(\theta_i - \theta_k) \right], \tag{2.54}$$

for $i = 1, 2, \ldots, m$.

The power balance equations for non-generator buses are given by:

$$P_{L_i}(V_i) + \sum_{k=1}^{n} V_i V_k \left[G_{ik} \cos(\theta_i - \theta_k) + B_{ik} \sin(\theta_i - \theta_k) \right] = 0, \tag{2.55}$$

$$Q_{L_i}(V_i) + \sum_{k=1}^{n} V_i V_k \left[G_{ik} \sin(\theta_i - \theta_k) - B_{ik} \cos(\theta_i - \theta_k) \right] = 0, \tag{2.56}$$

for $i = m + 1, m + 2, \ldots, n$, where , n is the total number of buses in the system and $Y_{ik} = G_{ik} + jB_{ik}$ the element of the i^{th} row and k^{th} column of the bus admittance matrix Y.

2.10.23 Power System Modeling

Power system modeling requires the modeling of all system components including, generators, transmission lines, transformers, loads and other control devices/systems, as discussed above. A complete power system modeling approach involves forming the overall system equations in the form of DAEs as:

$$\dot{x} = f(x, z, p), \tag{2.57}$$

$$0 = g(x, z, p), \tag{2.58}$$

where x is the vector of state variables, z the vector of algebraic variables and p the vector of system parameters. The differential equation set includes the dynamics of generators, excitation systems, load dynamics, and the algebraic equation set includes load flow equations and other algebraic relationship among the system components.

In power system modeling studies, the parameter values are chosen as either fixed values or within a certain range because the measurement of actual system parameters is very difficult. In particular, the load parameter values are difficult to obtain due to the large number of load components, the inaccessibility of certain customer loads, load compensation variations and the uncertainties of many load component characteristics.

2.11 Chapter Summary

The basic ideas about voltage instability and the importance of voltage instability analysis are explained from a fundamental as well as practical point of view in this chapter. The main focus of the chapter is to provide underlying causes of voltage instability, and the identification of different categories of stability behaviours that are important in power system stability analysis. The methods of improving voltage stability are also outlined.

In addition, this chapter discusses the dynamic modeling of a large power system. To provide a reliable model for implementation in a standard simulation tool, several factors must be taken into account. The first important process is to clearly define the purpose of the study. Each type of power system study requires a particular frequency bandwidth and a simulation time-frame depending on how fast the system dynamics needs to be investigated. Subsequently, the nature of the system being modelled must be carefully understood and the simulation tool used to simulate the models must be appropriately utilised.

Linear feedback control in power systems has a long history in terms of research and application. Linear controllers are preferred over nonlinear controllers because they impose lower requirements on practical implementation. However, as power system components are nonlinear in order to design a linear controller, linear models of a nonlinear system are needed. Different linearisation and modal analysis techniques will be discussed in the next chapter.

References

1. Vassell GS (1991) Northeast blackout of 1965. IEEE Power Eng Rev 11(1): 4–8
2. Lu W, Besanger Y, Zamai E, Radu D (2006) Blackouts: description, analysis and classification. In: 6th WSEAS international conference on power systems, pp 429–434
3. Custem TV, Vournas CD (1998) Voltage stability of the electric power systems. Kluwer Academic, Norwell
4. Berizzi A (2004) The Italian 2003 blackout. In: IEEE power engineering society general meeting, Denver, CO, pp 1673–1679
5. Ohno T, Imai S (2006) The 1987 Tokyo blackout. In: IEEE PES power systems conference and exposition, Atlanta, GA, pp 314–318
6. Andersson G, Donalek P, Farmer R, Hatziargyriou N, Kamwa I, Kundur P (2005) Causes of the 2003 major grids blackouts in North America and Europe, and recommendationed means to improve system dynamic performance. IEEE Trans Power Syst 20(4): 1922–1928
7. U.S. Canada Power System Outage Task Force (2004) Final report on the Aug 14 2003 blackout in the United States and Canada: causes and recommendations
8. Gao B, Morison GK, Kundur P (1996) Towards the development of a systematic approach for voltage stability assessment of large-scale power systems. IEEE Trans Power Sys 11(3): 1314–1324
9. Hossain MJ, Pota HR, Ugrinovski V (2008) Short and long-term dynamic voltage instability. In: 17th IFAC World Congress, Seoul, Korea, pp 9392–9397
10. IEEE (1990) Special publication 90TH0358-2-PWR: voltage stability of power systems: concepts, analytical tools, and industry experience

11. Vournas CD, Sauer PW, Pai MA (1996) Relationships between voltage and angle stability of power systems. Int J Electr Power Energy Syst 18(8): 493–500
12. Chi Y, Liu Y, Wang W, Dai H (2006) Voltage stability analysis of wind farm integration into transmission network. In: International conference on power system technology, pp 1–7
13. Lei Y, Mullane A, Lightbody G, Yacamini R (2006) Modeling of the wind turbine with a doubly-fed induction generator for grid integration studies. IEEE Trans Energy Convers 21(1): 257–264
14. Morison GK Gao B, Kundur P (1993) Voltage stability analysis using static and dynamic approaches. IEEE Trans Power Syst 8(3): 1159–1171
15. Taylor CW (1994) Power system voltage stability. McGraw-Hill, New York
16. Cutsem TV, Vournas C (1998) Voltage stability of electrical power system. Kluwer Academic, Norwell
17. Cutsem TV (2000) Voltage instability: phenomenon, countermeasures and analysis methods. Proc IEEE 88(2): 208–227
18. Kundur P (1994) Power system stability and control. Mcgraw-Hill, New York
19. Cutsem TV, Mailhot R (1997) Validation of a fast voltage stability analysis method on the Hydro-Quebec system. IEEE Trans Power Syst 12(1): 282–292
20. Ainsworth JD, Gavrilovic A, Thanawala HL (1980) Static and synchronous compensators for HVDC transmission convertors connected to weak AC systems. In: 28th session CIGRE, pp 31–41
21. Molinas M, Suul JA, Undeland T (2008) Low voltage ride through of wind farms with cage generators: STATCOM versus SVC. IEEE Trans Power Electr 23(3): 1104–1117
22. Molinas M, Suul JA, Undeland T (2006) Wind farms with increased transient stability margin provided by a STATCOM. In: IEEE 5th international conference on power electronics and motion control, pp 1–7
23. Pal B, Chaudhuri B (2005) Robust control in power systems. Springer, USA
24. Bergen AR (1986) Power system analysis. Prentice-Hall, New Jersey
25. Das JC, Casey J (1999) Effects of excitation controls on operation of synchronous motors. In: IEEE industrial and commercial power systems technical conference, Sparks, NV, pp 1–5
26. Klein M, Rogers GJ, Kundur P (1991) A fundamental study of inter-area oscillations in power systems. IEEE Trans Power Syst 6(3): 914–921
27. IEEE Committee Report (1981) Excitation system models for power system stability studies. IEEE Trans Power Apparatus Syst PAS 100(2): 494–509
28. Rogers G (2000) Power system oscillations. Kluwer Academic Publishers, Boston
29. Hill DJ (1993) Nonlinear dynamic load models with recovery for voltage stability studies. IEEE Trans Power Syst 8(1): 166–176
30. Ackermann T (2005) Wind power in power systems. Wiley, England
31. Li H, Chen Z (2008) Overview of different wind generator systems and their comparisons. IET Renew Power Gener 2(2):123–138
32. Morren J, de Haan SWH (2005) Ride-through of wind turbines with doubly-fed induction generator during a voltage dip. IEEE Trans Energy Convers 20(2): 435–441
33. Permitting of Wind Energy Facilities (2002) A handbook prepared by National Wind Coordinating Committee (NWCC) Siting Subcommittee, Aug 2002
34. Nandigam K, Chowdhury BH (2004) Power flow and stability models for induction generators used in wind turbines. In: IEEE power engineering society general meeting, Denver, CO, pp 2012–2016
35. Abdin ES, Xu W (2000) Control design and dynamic performance analysis of a wind turbine-induction generator unit. IEEE Trans Energy Convers 15(1): 91–96
36. Akhmatov V, Knudsen H (2002) An aggregate model of a grid-connected, large-scale, offshore wind farm for power stability investigations-importance of windmill mechanical system. Int J Electr Power Energy Syst 24(9): 709–717
37. Akhmatov V, Knudsen H, Nielsen A (2000) Advanced simulation of windmills in the electrical power supply. Int J Electr Power Energy Syst 22(6): 421–434

38. Feijo A, Cidrs J, Carrillo C (200) A third order model for the doubly-fed induction machine. Electric Power Syst Res 56(2): 121–127
39. Ledesma P, Usaola J, Rodriguez JL (2003) Transient stability of a fixed speed wind farm. Renew Energy 28(9): 1341–1355
40. Mahmud MA, Pota HR, Hossain MJ (201)2 Dynamic stability of three-phase grid-connected photovoltaic system using zero dynamic design approach. IEEE J Photovoltaics 12(4): 564–571
41. Mahmud MA, Pota HR, Hossain MJ (2011) Modeling guidelines and a benchmark for power system simulation studies of three-phase single-stage photovoltaic systems. IEEE Trans Power Deliv 26(2): 1247–1264
42. Tan YT, Kirschen DS, Jenkins N (2004) A model of PV generation suitable for stability analysis. IEEE Trans Energy Convers 19: 748–755
43. Nosrat A, Pearce, J.M.: Dispatch strategy and model for hybrid photovoltaic and tri-generation power systems. Appl Energy 88(9): 3270–3276
44. Hingorani MG, Gyugyi L (2000) Understanding FACTS: concepts and technology of flexible AC transmission systems. IEEE Press, New York
45. Divya KC, Ostergaard J (2009) Battery energy storage technology for power systems—an overview. Electric Power Syst Res 79(4): 511–520
46. Acha E, Fuerte-Esquivel CR, Ambriz-Perez H, Angles-Camacho C (2004) FACTS modeling and simulation in power networks. Wiley, London
47. Karasik V, Dixon K, Weber C, Batchelder B, Campbell G, Rebeiro P (1999) SMES for power utility applications: a review of technical and cost considerations. IEEE Trans Appl Supercond 9(2): 541–546
48. Lasseter RH, Jalali SG (1991) Power conditioning systems for superconductive magnetic energy storage. IEEE Trans Energy Convers 6(3): 381–387
49. Varakin IN, Klementov AD, Litvinenko SV, Starodubtsev NF, Stepanov AB (1997) Application of ultracapacitors as traction energy sources. In: Proceedings of 7th international seminar on double layer capacitors and similar energy storage devices, Florida, USA

http://www.springer.com/978-981-287-115-2

Robust Control for Grid Voltage Stability: High Penetration of Renewable Energy
Interfacing Conventional and Renewable Power Generation Resources
Hossain, J.; Pota, H.R.
2014, XVIII, 311 p. 164 illus., 10 illus. in color.,
Hardcover
ISBN: 978-981-287-115-2